A Molecular Dynamics Investigation of Rare-Gas Solvated Cation−Benzene Clusters Using a New Model Potential

M. Albertí,[†] A. Castro,[‡] A. Laganà,*[,‡] M. Moix,[‡] F. Pirani,[‡,||] D. Cappelletti,[§,||] and G. Liuti[§]

Departament de Química Física i Centre de Recerca en Química Teòrica, Parc Científic, Universitat de Barcelona, Martí i Franquès, 1, 08028 Barcelona, Spain, and Dipartimento di Chimica, Dipartimento di Ingegneria Civile ed Ambientale, Università di Perugia, 06123 Perugia, Italy

Received: November 2, 2004

The main static and dynamic properties of some ionic heteroclusters, involving K^+, C_6H_6, and Ar, have been investigated. A new representation of the intermolecular potential energy, which takes into account both electrostatic and non-electrostatic contributions to the overall noncovalent interaction, was used. Dynamical calculations were performed for a microcanonical ensemble. Particular attention was paid to the opening of the isomerization and dissociation processes for $K^+-C_6H_6-Ar_n$ and to the formation of some of its fragments at increasing temperatures of the cluster considered.

1. Introduction

Noncovalent intermolecular interactions[1] play an important role in several physical, chemical, and biochemical processes. In recent times, particular attention has been paid to molecular aggregates involving aromatic rings for which noncovalent intermolecular interactions control basic phenomena such as the formation of weak hydrogen bonds[1,2] and the competitive solvation of ions by different partners,[3−5] as well as molecular recognition and selection processes.[6−8] These phenomena are typically governed by the combination of various components of the noncovalent intermolecular interaction like electrostatic (of either attractive or repulsive nature), exchange or size (of repulsive nature), and induction and dispersion (of attractive nature). In certain cases, as in the alkaline-earth-dication−benzene systems, charge-transfer components also come into play to open the reactive channels at the conical intersection between different potential energy surfaces.

Unfortunately, it is quite difficult to accurately characterize the relative role played by the various components of noncovalent intermolecular interactions and give a proper formulation to their dependence on the intermolecular distance and on the geometry of the molecular aggregate, because they are, in general, much weaker than those leading to the usual chemical bonds. Nonetheless, it is worth spending significant theoretical and experimental efforts on their detailed determination so as to found the modeling on solid molecular science fundamentals.

For this reason, research activity on molecular aggregates involving aromatic molecules has significantly increased in recent times.[6−36] For the same reason, we are spending significant efforts to investigate the alkaline-ions−benzene−rare-gas systems. Examples of experimental work aimed at estimating the stabilization energy of weakly bound complexes are given in refs 14 and 15. In particular, the development of pulsed supersonic molecular beam techniques has allowed detailed spectroscopic investigations of various series of van der Waals complexes consisting of aromatic molecules and polarizable solvents.[14] A specific discussion of the microsolvation of benzene by rare-gas atoms is given in refs 12, 14, 17, and 18. Molecular dynamics simulations of the van der Waals complexes involving aromatic molecules have also been performed[25−29] to provide useful means for razionalizing the structure, the formation, the internal energy relaxation, the solvent perturbation, and the energy partitioning of these systems.

A theoretical study of the electronic energy of the van der Waals complexes of aromatic molecules has also been carried out. The cation−π-electrons interaction of these systems is characterized by a strong electrostatic component.[6−9,31,33] However, a description of the interaction in terms of a pure electrostatic component only provides a qualitative picture of the situation for simple cation−aromatic-electrons clusters.[31,32] In fact, as already mentioned, a complete, quantitative description of the noncovalent interaction can only be worked out by incorporating further ingredients such as the exchange, dispersion, and induction components.[7−10] Unfortunately, in this respect, the experimental information is limited to the formation enthalpy[6,7] and the binding energy,[11] while the theoretical information is limited to the most stable configuration (see, for example, refs 9 and 10). For this reason, we spent a significant amount of work to characterize more quantitatively the cation−π aromatic interaction and find the most appropriate formulation of its various components by considering as a case study the K^+−benzene aggregate and its solvated K^+−benzene−Ar_n ($n = 1, 2, 3$) form. This work, the results of which are discussed in the present paper, is part of a more general effort to extend interaction models to large systems after validating them on fairly simple ones.

The paper is articulated as follows: In section 2, we discuss the formulation of the potential energy surface (PES), and in section 3, we discuss the main dynamical properties of these systems using the molecular dynamics program DL_POLY.[37] Concluding remarks are given in section 4.

2. Potential Energy Surface of the K^+−Benzene and K^+−Benzene−Ar_n Clusters

The description of the interactions for the title molecular systems was obtained by gathering together the outcome of some

* Corresponding author. Electronic mail: lag@unipg.it.
[†] Universitat de Barcelona.
[‡] Dipartimento di Chimica, Università di Perugia.
[§] Dipartimento di Ingegneria Civile ed Ambientale, Università di Perugia.
[||] Also at I. N. F. M., Unità di Perugia.

10.1021/jp0450078 CCC: $30.25
Published on Web 03/04/2005

ab initio calculations and the information derived from extended *empirical* and *semiempirical* studies. Ab initio calculations, performed for the alkaline ion−π complexes,[9,10] indicate that accurate potential energy values can be obtained only by carrying out high-level quantum mechanical basis sets and that induction is sometimes a significant source of attraction. It has also been shown that the inclusion of nonadditive effects can be important to the end of obtaining a correct estimate of the binding energy of cation−benzene systems.[35] The ab initio calculations also indicate that the binding energy decreases by about a factor 3 along the alkaline ion series, while the equilibrium distance increases by about a factor 2.[9,10] This information, which refers only to the most stable geometry of the complex, agrees with the experimental findings.[11]

Yet, as already mentioned, for a complete investigation of the properties of the system, an accurate description of the whole PES is needed. This makes it important to adopt a functional representation of the potential that is properly expressed in terms of the leading components of the interaction, that directly applies to the alkaline ion series mentioned already and that can be easily generalized to systems with increasing complexity.

In this paper, the intermolecular interaction is formulated as arising from the combination of a (size) *repulsion* component and an (induction and dispersion) *attraction* component.

This combination of components is usually termed non-electrostatic potential (V_{nel}), as opposed to the electrostatic one (V_{el}) that is the other component of the overall (V_{total}) interaction.

2.1. The Non-Electrostatic Component. The non-electrostatic component V_{rel} of the potential includes ion (atom)−molecule potentials (V_{K^+-bz} and V_{bz-Ar}, respectively), each one taken as a sum of 12 ion (atom)−bond interaction terms of the type[38]

$$V(r,\alpha) = \epsilon(\alpha)\left[\frac{m}{n(r,\alpha)-m}\left(\frac{r_m(\alpha)}{r}\right)^{n(r,\alpha)} - \frac{n(r,\alpha)}{n(r,\alpha)-m}\left(\frac{r_m(\alpha)}{r}\right)^{m}\right] \quad (1)$$

Such a simple formulation provides a realistic picture of both repulsion and attraction. It also indirectly incorporates the three body effects,[38] leads to a proper description of nonequilibrium geometries of the cluster,[39] and could be conveniently used in dynamical calculations. In eq 1, r is the distance of the ion (atom) from the bond center, and α is the angle that r forms with the bond considered. The parameter m is set equal to 4 for the K^+−bond interactions and equal to 6 for the Ar−bond interactions. The parameter n that defines the falloff of the ion (atom)−bond repulsion is expressed as a function of both r and α using the equation

$$n(r,\alpha) = \beta + 4.0\left(\frac{r}{r_m(\alpha)}\right)^2 \quad (2)$$

where $\beta = 10.0$ for both Ar− and K^+−bond interactions.[38] The other important parameters of the potential ϵ and r_m (representing, respectively, the well depth and the equilibrium distance of the relevant ion (atom)−bond pair) are assumed to depend on α according to the relationships

$$\epsilon(\alpha) = \epsilon_\perp \sin^2(\alpha) + \epsilon_{||}\cos^2(\alpha) \quad (3)$$

$$r_m(\alpha) = r_{m\perp}\sin^2(\alpha) + r_{m||}\cos^2(\alpha) \quad (4)$$

The ion (atom)−bond model potential of eq 1 is also used to describe the K^+−Ar and Ar−Ar interactions (V_{K^+-Ar} and V_{Ar-Ar}, respectively) by suppressing the angular dependence of ϵ and r_m.

TABLE 1: Cation (Atom)−Bond Interaction Parameters

atom....bond	$\epsilon_\perp$/meV	$\epsilon_{||}$/meV	$r_{m\perp}$/Å	$r_{m||}$/Å	m
K^+....C−C	22.95	75.77	3.266	3.547	4
K^+....C−H	39.97	42.70	3.044	3.240	4
Ar....C−C[a]	3.895	4.910	3.879	4.189	6
Ar....C−H[a]	4.814	3.981	3.641	3.851	6

[a] Same values as in ref 38.

TABLE 2: Cation (Atom)−Atom Interaction Parameters

atom .... atom	ϵ/meV[a]	r_m/Å[a]	m
Ar .... K^+	110.0	3.190	4
Ar .... Ar	12.34	3.760	6

[a] Same values as in refs 40 and 49.

All the parameters necessary to describe the components of the K^+−benzene−Ar_n cluster interaction are given in Tables 1 and 2. Quoted values for ϵ and r_m were derived using the charge and the polarizability of the related atomic species as well as polarizability and effective polarizability tensor components of aromatic C−C and C−H bonds, assumed to have an ellipsoidal shape whose center approximately coincides with that of the bond.[38,42]

The procedure, described in detail for atom−bond,[42] is extended in this paper for the first time to ion−bond. This formulation of the potential also accounts for nonadditive effects via a controlled decrease of the polarizability values with respect to their values in isolated molecules.[35]In more detail, the polarizability values used for the calculations are 0.85 Å^3 for K^+,[40] 1.64 Å^3 for Ar,[41] 2.25 and 0.48 Å^3 for the parallel and perpendicular components of C−C as well as 0.79 and 0.58 Å^3 for the same components of CH.[43] The latter bond components are reduced by 15% and those of C−C by approximately 20% to account for nonadditive effects in the ion−benzene interaction.[35]

2.2. The Electrostatic Component. The electrostatic component V_{el} that in the present case asymptotically corresponds to the ion quadrupole interaction is formulated, as suggested previously, as a sum of Coulombic potentials.[44,45] These potentials are associated with the interaction of K^+ and both the negative charges (placed on the C atoms of the benzene on both sides of the aromatic ring) and the positive charges (placed on the H atoms of the benzene). The sizes of the charges and their positions are chosen to reproduce the correct components of the benzene quadrupole moment.[46,47] The procedure leads to a charge of +0.092 45 on each H atom and to two negative charges of −0.046 23 separated by 1.905 Å on each carbon atom. Accordingly, the overall K^+−benzene−Ar_n interaction, V_{total}, is formulated as

$$V_{total} = V_{K^+-bz} + \sum_{i=1}^{n} V_{bz-Ar_i} + \sum_{i=1}^{n} V_{K^+-Ar_i} + \sum_{i=1}^{n-1}\sum_{j>i}^{n} V_{Ar_i-Ar_j} + V_{el} \quad (5)$$

where bz indicates the benzene and the index *i(j)* indicates that the contribution is associated with the *i*th(*j*th) Ar atom. Therefore, the resulting global PES not only reproduces the diatomic asymptotic properties (like those of the K^+−Ar and Ar−Ar pairs but also provides direct information on the properties of the K^+−benzene system that will be discussed in the next section using molecular dynamics means.

3. The Molecular Dynamics Investigation

As already mentioned, molecular dynamics investigations were carried out using the DL_POLY suite of programs.[37] The aim of the study was to further analyze the characteristics of the proposed PES through the rationalization of the dynamic behavior of the K^+−benzene and K^+−benzene−Ar_n clusters ($n = 1, 3$).

3.1. The Calculations. To carry out the dynamical calculations, a fortran routine, returning the value of the adopted PES and the values of the related derivatives with respect to the internuclear distances, was assembled. The initial conditions of the system were set to correspond to a microcanonical ensemble (*NVE*) of particles and various (increasing) values of the total energy (E_{total}, i.e., the sum of the potential and kinetic energy of the cluster). As in previous studies,[29,38,39] the benzene molecule was treated as a rigid body. At each new energy, calculations were started by taking as the initial configuration of velocities and forces the final values of the previous run. A time step of 1 fs was adopted for the integration of the motion equations. This value was found to be short enough to ensure a relative fluctuation of the total energy smaller than 10^{-5}. The instantaneous temperature T was calculated at each time step from the kinetic energy E_k by means of the relationship $T = 2E_k/k_B f$ (with k_B being the Boltzmann constant and f the number of degrees of freedom in the system). The total integration time for the simulations was generally set at 25 ns, except for the cases in which cluster interconversions were observed. In these cases, the integration time was extended to 100 ns. Calculations were performed by imposing no restrictions on the neighboors and by evaluating the interaction at every time step for all ion (atom)−bond pairs. Finally, to properly assess the results obtained for each cluster (see the following sections), it is useful to introduce the configuration energy (E_{cfg}) of the cluster that is defined as an average of V_{total} over all the accessible configurations at the chosen total energy. By using this method, E_{cfg} can be decomposed either as a sum of the electrostatic (E_{el}) and the non-electrostatic (E_{nel}) components or as a sum of asymptotic fragments energy: E_{K^+-bz}, E_{bz-Ar_i}, and $E_{K^+-Ar_i}$.

3.2. The K^+−Benzene Clusters. The first phase of the investigation was concerned with the study of the structural and energetic properties of the K^+−benzene clusters. The contours of V_{total} for this system are shown in Figure 1.

As is apparent from the figure, the most stable structure of the cluster is the one in which the K^+ ion sits on the C_{6v} symmetry axis of the aromatic ring. The value of V_{total} of the cluster in this arrangement (−927 meV) is mainly determined by the electrostatic component (−635.6 meV) evaluated at the equilibrium distance (2.69 Å away from the benzene center of mass). This value accounts, in fact, for about 70% of the total intermolecular energy. The non-electrostatic component V_{nel}, calculated under the same conditions as the sum of the twelve cation−bond interactions (six K^+−CC and six K^+−CH), accounts for the remaining part of V_{total}. It is worth pointing out here that the most stable geometry, binding energy, and equilibrium distance predicted by the model are in agreement with the ab initio results[9,10,35,36,48,49] and the experimental findings.[11,45] Moreover, in addition, the estimate of the relative importance of the induction and electrostatic components falls within the uncertainty of the theoretical predictions.[9,10]

Six equivalent isomers are generated when K^+ is placed on the same plane of the aromatic ring. These isomers are less stable than the previously mentioned arrangement in which the K^+ ion sits on the C_{6v} symmetry axis of benzene. The large energy difference between the two types of arrangement (in- and out-of-plane) makes interconversions between the different isomers quite unlikely. Moreover, a large dissociation probability should be expected when the cluster ends up being coplanar.

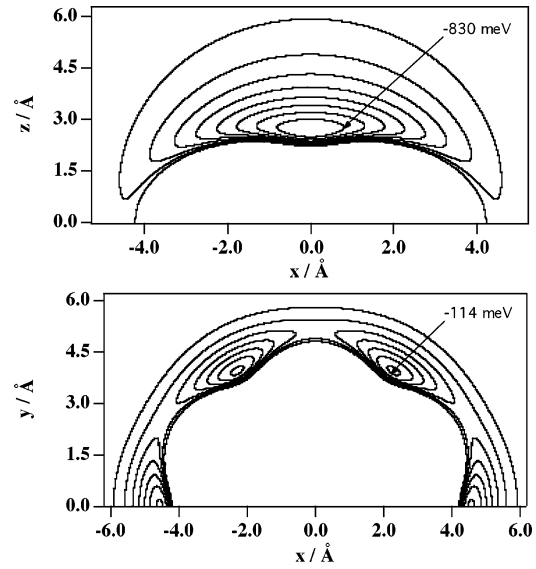

Figure 1. Isoenergetic contours of the potential energy surface of the K^+−benzene system. The benzene molecule lies on the *xy* plane. The K^+ ion approaches the benzene center of mass either (see the upper panel) perpendicularly to the center of mass along the *z* axis (i.e., along the C_{6v} axis of symmetry) or on-plane (see the lower panel). Energy contours are spaced by 100 meV in the upper panel and by 15 meV in the lower panel.

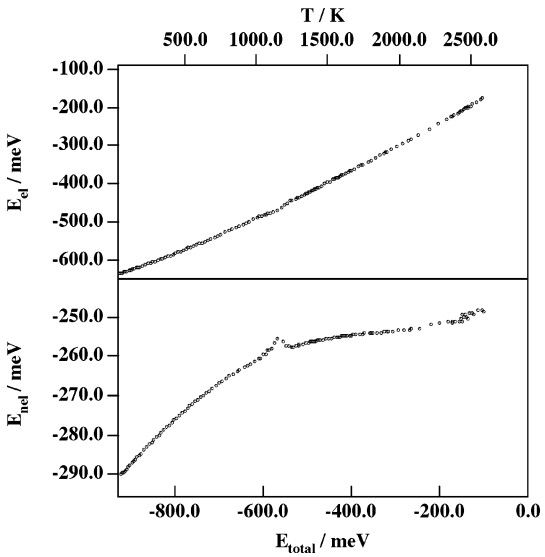

Figure 2. The variation of E_{el} (upper panel) and E_{nel} (lower panel) components plotted as a function of E_{total} and T.

The variation of both E_{el} and E_{nel} with E_{total} (and, consequently, with the temperature) are plotted in the upper and lower panels, respectively, of Figure 2. As is apparent from the figure, the E_{el} curve increases more rapidly than that for the non-electrostatic contribution. As a matter of fact, the percentage of E_{el} in E_{cfg} varies from 68.7% to 41.4% when approaching dissociation.

A peculiar feature of the plots is that they show a clear change of slope at about $E_{total} = -600$ meV. In the case of the non-electrostatic component, the change is accompanied by a knee. This indicates that the exploration of a region of increasing repulsion of the relevant PES results in the opening of a channel

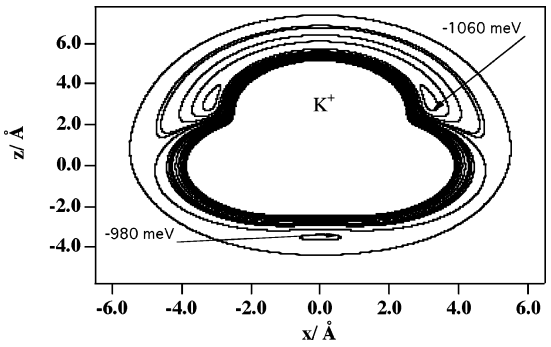

Figure 3. Isoenergetic curves for the K^+−benzene−Ar cluster. The K^+−benzene is kept fixed at its equilibrium geometry. The Ar atom is allowed to move around on the *xz* plane. Energy contours are spaced by 25 meV with the curves taken at −980 meV (isomer (1|1) individually labeled.

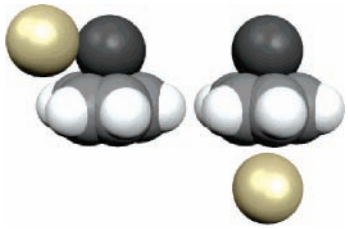

Figure 4. A sketch of the (2|0) (left-hand side) and (1|1) (right-hand side) isomers of the K^+−benzene−Ar cluster.

TABLE 3: Properties of K^+−Benzene−Ar Clusters[a]s

isomer	R1/Å	R2/Å	θ/deg	V_{el}/meV	V_{nel}/meV
(2|0)	2.689	4.418	44.0	−636	−429
(1|1)	2.690	3.510	180.0	−636	−346

[a] R1 = distance of K^+ from the benzene center of mass, R2 = distance of Ar from the benzene center of mass, θ = angle formed by R1 and R2), V_{el} = electrostatic energy, and V_{nel} = non-electrostatic energy for both the (2|0) and the (1|1) isomers.

associated with a wide region of previously unaccessed fairly stable configurations. This not only reduces the tendency of the system to dissociate but also slows down the pace by which energy increases.

3.3. The K^+−Benzene−Ar Clusters. The interaction between Ar and K^+ is stronger than that between two Ar atoms or that between Ar and benzene. This makes the Ar atom tend to condense about the cation. The isoenergetic contours for the K^+−benzene−Ar cluster are shown in Figure 3. The contours are taken by placing the benzene molecule on the *xy* plane and by putting the K^+ ion at the equilibrium position. The Ar atom is allowed to move on the *xz* plane.

The figure shows that the most stable cluster structure is the (2|0) one for which both Ar and K^+ sit on the same side with respect to the molecular plane of C_6H_6 (though, the (1|1) structure also, in which K^+ and Ar stay on opposite sides of the benzene plane, is stable). The structure of these two isomers is illustrated in Figure 4, and their geometric and energetic parameters are given in Table 3.

The two isomers are separated by a small energy barrier of about 100 meV (see Figure 3). This means that above a certain temperature interconversions between the two isomers are quite likely. This is, indeed, confirmed by dynamical calculations: when the kinetic energy becomes sufficiently large to allow the system to surmount the barrier (though being still too small to induce dissociation), interconversions come into play. However, contrary to what happens for the benzene−Ar_n clusters, the time

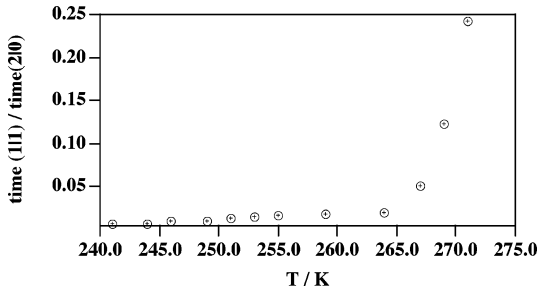

Figure 5. Isomeric distribution of the K^+−benzene−Ar cluster given as the ratio between the amount of time spent by the cluster in the (1|1) configuration and that spent in the (2|0) one plotted as a function of the temperature *T*.

spent by the cluster in the (2|0) configuration is much longer than that spent in the configuration (1|1). The evolution of the isomeric population (defined as the ratio of the time spent by the cluster in configuration (1|1) divided by that spent in configuration (2|0) is illustrated in Figure 5 where it is plotted as a function of the temperature, *T*.

As in other dynamical studies concerned with the benzene−Ar_2 clusters,[25,39] the criterion adopted to decide whether an interconversion between the two isomers has taken place is that the isomer is required to remain around a particular geometry for at least 5 ps. No interconversions have been observed at temperatures lower than 240 K. From 240 to 264 K, the number of interconversions increases from 4 to 64, but the isomeric population for the (1|1) isomer is always lower than 2%. This population increases at higher temperatures, about 24% at 271 K. However, at these high temperatures, the probability of dissociating into Ar + K^+−benzene also increases. For example, at 271 K, the cluster already dissociates after only 15 ns. At temperatures higher than 300 K, the K^+−benzene−Ar cluster becomes highly unstable.

The changes observed for some contributions of the interaction energy of the K^+−benzene−Ar clusters as the total energy increases (because of the heating of the cluster) are shown in Figure 6.

The figure shows that when E_{total} varies from −1065.0 to −920.69 meV (an increase of about 70 meV of kinetic energy) the increase of the K^+−benzene and K^+−Ar energy interactions are 4% and 20%, respectively.

The most important increase is that of benzene−Ar, for which the fraction of binding energy lost before dissociation was found to be about 45%. As is apparent from the figure, the K^+−benzene energy depends linearly on E_{total}, while the slopes of both K^+−Ar and benzene−Ar energies change at about $E_{total} = -960$ meV. This marks the beginning of the isomeric interconversion regime. When isomerization occurs, the distance of Ar from K^+ and benzene increases, leading to a sudden weakening of the stability of the relevant bonds. Moreover, the access to a larger number of benzene−Ar configurations makes the associated energy remain nearly constant. At the highest values of the temperature at which the population of isomer (1|1) increases sharply (see Figure 5), the energy associated with the benzene−Ar interaction rises to values which lead to the dissociation of the Ar atom. Figure 7 shows the evolution during 25 ns of the simulation trajectory of both the K^+−Ar distance and the V_{K^+-Ar} component of the interaction at −922 meV of the total energy. As shown by these plots, despite the increase of the E_{K^+-Ar} energy (see Figure 6) when the isomerization occurs, the cluster spends much more time in the most stable configurations (lower energies and distances) along the trajectory.

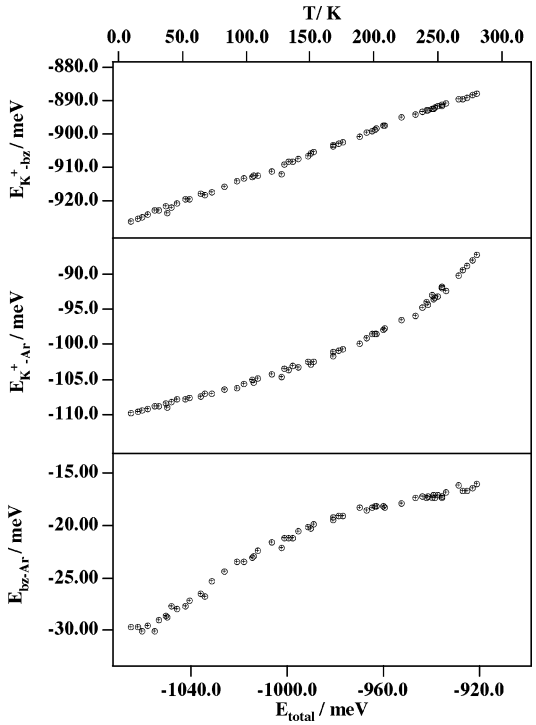

Figure 6. The contributions E_{K^+-bz}, E_{K_+-Ar}, and E_{bz-Ar} of E_{cfg} of the K^+−benzene−Ar cluster plotted as a function of E_{total} and T.

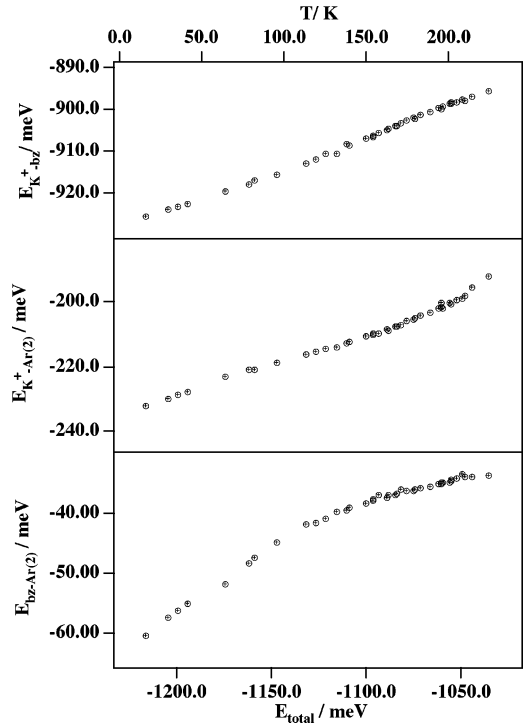

Figure 8. The components E_{K^+-bz}, E_{K^+-Ar}, and E_{bz-Ar} of E_{cfg} of the K^+−benzene−Ar_2 cluster plotted as a function of E_{total} and T.

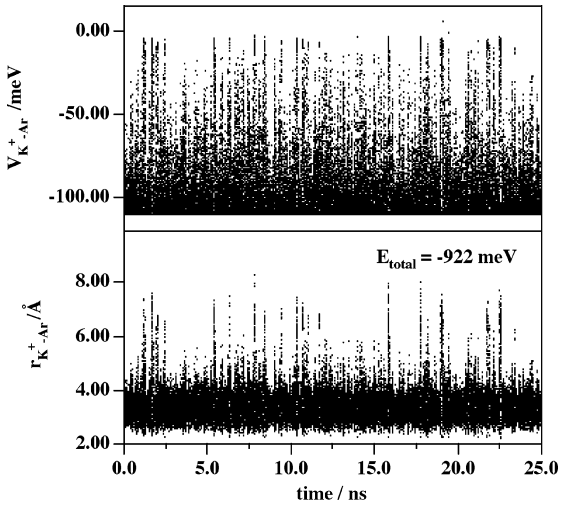

Figure 7. Time evolution of the K^+−Ar interaction energy (upper panel) and K^+−Ar distance (lower panel) during a 25-ns simulation at $E_{total} = -922$ meV.

3.4. The K^+−Benzene−Ar_n ($n = 2, 3$) Clusters. For clusters containing more than one Ar atom, the most stable structures are those for which K^+ and the rare gas atoms lie on the same side with respect to the plane of the aromatic ring. When the kinetic energy becomes sufficiently large, other fairly stable structures can be obtained, although the time spent by the atoms of the cluster in arrangements in which K^+ and the Ar atoms are placed on the same side with respect to the aromatic ring is much larger than that spent in configurations in which the Ar atoms are distributed on both sides. Moreover, for clusters made of two or more Ar atoms, the dissociation becomes a highly probable event when they isomerize. This means that the K^+−Ar interaction plays a key role in stabilizing the K^+−benzene−Ar_n heteroclusters. As a matter of fact, only those configurations for which the K^+−Ar interaction stabilizes the system allow the benzene−rare-gas aggregate to live long enough to consider the cluster formed. The K^+−benzene−Ar_3 and the K^+−benzene−Ar_3 clusters dissociate at about 220 and 200 K, respectively. The corresponding dissociation products are K^+−benzene−Ar + Ar and K^+−benzene−Ar_2 + Ar, respectively. Figure 8 illustrates the variation of the different contributions to the interaction energy for the K^+−benzene−Ar_2 clusters as the total energy increases.

As is apparent from the figure, the plots corresponding to the various contributions have the same qualitative behavior as those of the K^+−benzene−Ar cluster (see Figure 6). The main difference lies in the interval of temperature in which interconversions are observed. For the K^+−benzene−Ar clusters, interconversions occur between $T = 240$ and 280 K, while for the K^+−benzene−Ar_2 clusters, interconversions occur between $T = 180$ and 220 K. However, as has been already pointed out, a high dissociation probability is associated with the isomerization of the K^+−benzene−Ar_2 cluster. A similar behavior is observed for the K^+−benzene−Ar_3 cluster, which tends to fragment into K^+−benzene−Ar_2 at temperatures above 200 K. The different contributions to the interaction energy as a function of total energy show the same qualitative tendency as that of K^+−benzene−Ar and K^+−benzene−Ar_2 clusters. Despite the fact that interconversions between the possible isomers can occur between 170 and 190 K, the simulations indicate that the K^+−benzene−Ar_3 cluster keeps the three Ar atoms on the same side of the K^+ ion with respect to the benzene plane.

This is true even when one of the Ar atoms is loosely bound to benzene, because it sits on top of the K^+ ion. These results show once more the importance of the K^+−Ar interaction in determining the properties of the K^+−benzene−Ar_n family of clusters. The cation remains bound to the organic compound, and the Ar atoms move preferentially around the K^+ ion. In other words, a kind of self-cavity forms in which the ion remains confined while moving concertedly with the Ar atoms. However, as has already been noted, the Ar atoms are able to easily move far away. In this sense, the K^+−benzene−Ar_n cluster can be understood as a K^+−benzene cluster solvated by Ar atoms (that

can also easily desolvate). The ability of the aromatic rings to coordinate a cation has been proven[8,50] from resolution crystal structure. Here, the focus has been put, however, on the fact that the dominant interaction in the K^+−benzene−Ar_n clusters corresponds to the K^+−benzene one. This, together with the fact that the Ar atoms move easily around the K^+ ion, allows us to think that when the K^+ ions are solvated by argon atoms in the presence of the aromatic ring the sphere of solvation can be opened to allow the cation to interact with the aromatic benzene.

4. Conclusions

This paper focuses on the problem of providing accurate descriptions of the interaction energies and molecular dynamics of weakly bound systems and is meant to contribute to the rationalization of the microscopic mechanisms leading to energy transformation in noncovalent molecular aggregates.[5,8] In this context, we have considered as a case study the K^+−benzene−Ar_n systems, and we have formulated the interaction of the cation−benzene−rare-gas aggregate (and that of its fragments) in terms of a new ion (atom)−bond functional representation. The discussion has shown that K^+ binds to the π electronic cloud of benzene with a strong noncovalent component which largely coincides with an electrostatic interaction between the positive ion and the quadrupole moment of the benzene. The study of the properties of the K^+−benzene system solvated by rare-gas atoms, performed using dynamical calculations, has singled out the importance of the ion in stabilizing the system and the key role it plays in condensing the rare gas atoms on the same side of the benzene. Moreover, the study has allowed us to rationalize the dynamics of the clusters by providing evidence that the Ar atoms tend to solvate the K^+ ion in a concerted way. This could give grounds to some of the mechanisms proposed in the literature to rationalize the behavior of ions in biological channels and has prompted the request for an investigation of the behavior of the corresponding anionic systems. Preliminary investigations undertaken in our laboratory for anionic rare-gas clusters seem, in fact, to offer additional hints on the ion mobility in aromatic systems and on the mechanisms which can pivot ion selectivity in biological channels.

Acknowledgment. M. Albertí acknowledges financial support from the Ministerio de Educación Cultura y Deporte (Programa para la movilidad de profesores Españoles y extranjeros: PR2002-0014), from the Spanish DGICYT (projects PB97-0919 and BQU2001-3018) and from the Generalitat de Catalunya (CUR 2001SGR-00041). EU support through the MCInet Research Training Network ("Generation, Stability and Reaction Dynamics of Multiply Charged Ions in the Gas Phase", contract HPRN-CT-2000-00027) and COST in Chemistry Action D23 is also acknowledged. The research has also been supported by MIUR, CNR, and ASI.

References and Notes

(1) Müller-Dethelfs, K.; Hobza, P. *Chem Rev.* **2000**, *100*, 143.
(2) Alonso, J. L.; Antolínez, S.; Bianco, S.; Lesarri, A.; López, J. C.; Caminati, W. *J. Am. Chem. Soc.* **2004**, *126*, 3244.
(3) Cabarcos, O. M.; Weinheimer, J. C.; Lisy, J. M. *J. Chem. Phy.* **1998**, *108*, 5151.
(4) Cabarcos, O. M.; Weinheimer, J. C.; Lisy, J. M. *Chem. Phys.* **1999**, *110*, 8429.
(5) Morais-Cabral, J. H.; Zhou, Y.; MacKinnon, R. *Nature (London)* **2001**, *414*, 37.
(6) Kumpf, R. A.; Dougherty, D. A. *Science* **1993**, *261*, 1708.
(7) Dougherty, D. A. *Science* **1996**, *271*, 163.
(8) Ma, J. C.; Dougherty, D. A. *Chem. Rev.* **1997**, *97*, 1303.
(9) Tsuzuki, S.; Yoshida, M.; Uchimaru, T.; Mikami, M. *J. Phys. Chem. A* **2001**, *105*, 769.
(10) Kim, D.; Hu, S.; Tarakeshwar, P.; Kim, K. S.; Lisy, J. M. *J. Phys. Chem. A* **2003**, *107*, 1228 and references therein.
(11) Amicangelo, J. C.; Armentrout, P. B. *J. Phys. Chem. A* **2000**, *104*, 11420.
(12) Ondrechen, J. M.; Berkovitch-Yellin, Z.; Jortner, J. *J. Am. Chem. Soc.* **1981**, *103*, 6586.
(13) Fried, L. E.; Mukamel, S. *J. Chem. Phys.* **1991**, *96*, 116.
(14) Schmidt, M.; Le Calvè, J.; Mons, M. *J. Chem. Phys.* **1993**, *98*, 6102 and references therein.
(15) Cappelletti, D.; Bartolomei, M.; Aquilanti, V.; Pirani, F. *J. Phys. Chem. A* **2002**, *106*, 10764.
(16) Pirani, F.; Porrini, M.; Cavalli, S.; Bartolomei, M.; Cappelletti, D. *Chem. Phys. Lett.* **2003**, *367*, 405.
(17) Mons, M.; Courty, A. M.; Le Calvè, J.; Piuzzi, F.; Dimicoli, I. *J. Chem. Phys.* **1997**, *106*, 1676.
(18) Easter, D. C.; Bailey, L.; Mellot, J.; Tirres, M.; Weiss, T. *J. Chem. Phys.* **1998**, *108*, 6135.
(19) Schmidt, M.; Mons, M.; Le Calvè, J. *Chem. Phys. Lett.* **1991**, *177*, 371.
(20) Brupbacher, Th.; Makarewicz, J.; Bauder, A. *J. Chem. Phys.* **1994**, *101*, 9736.
(21) Hobza, P.; Bludsky, O.; Selzle, H. L.; Schalg, E. W. *Chem. Phys. Lett.* **1996**, *250*, 402.
(22) Lenzer, T.; Luther, K. *J. Chem. Phys.* **1996**, *105*, 10944.
(23) Bernshtein, V.; Oref, I. *J. Chem. Phys.* **2000**, *112*, 686.
(24) Dykstra, C. E.; Lisy, J. M. *THEOCHEM* **2000**, *500*, 375.
(25) Vacek, J.; Konvicka, K.; Hobza, P. *Chem. Phys. Lett.* **1994**, *220*, 85.
(26) Vacek, J.;. Hobza, P. *J. Phys. Chem.* **1994**, *98*, 11034.
(27) Dullweber, A.; Hodges, M. P.; Wales, D. J. *J. Chem. Phys.* **1997**, *106*, 1530.
(28) Riganelli, A.; Memelli, M.; Laganà, A. *Lect. Notes Comput. Sci.* **2002**, *2331*, 926.
(29) Zoppi, A.; Becucci, M.; Pietraperzia, G.; Castellucci, E.; Riganelli, A.; Albertí, M.; Memelli, M.; Laganà, A. In *Clustering properties of rare gas atoms on aromatic molecules*; 16th International Symposium on Plasma Chemistry, Taormina, Italy June 22−27, 2003.
(30) Koch, H.; Fernández, B.; Makariewicz, J. *J. Chem. Phys.* **1999**, *111*, 198.
(31) Mecozzi, S.; West, A. P., Jr.; Dougherty, D. A. *Proc. Natl. Acad. Sci. U.S.A.* **1996**, *93*, 10566.
(32) Mecozzi, S.; West, A. P., Jr.; Dougherty, D. A. *J. Am. Chem. Soc.* **1996**, *118*, 2307.
(33) Felder, C.; Jiang, H.-L.; Zhu, W.-L., Chen, K.-X.; Silman, I.; Botti, S. A.; Sussman, J. L. *J. Phys. Chem. A* **2001**, *105*, 1326.
(34) Cubero, E.; Luque, F. J.; Orozco, M. *Proc. Natl. Acad. Sci. U.S.A.* **1998**, *95*, 5976.
(35) Caldwell, J. W.; Kollman, P. A. *J. Am. Chem. Soc.* **1995**, *117*, 4177.
(36) Nicholas, J. B.; Hay, B. P.; Dixon, D. A. *J. Phys. Chem. A* **1999**, *103*, 1394.
(37) http://www.dl.ac.uk/TCSC/Software/DL_POLY.
(38) Pirani, F.; Albertí, M.; Castro, A.; Moix, M.; Cappelletti, D. *Chem. Phys. Lett.* **2004**, *394*, 37.
(39) Albertí, M.; Castro, A.; Laganà, A.; Pirani, F.; Porrini, M.; Cappelletti, D. *Chem. Phys. Lett.* **2004**, *392*, 514.
(40) Cappelletti, D.; Liuti, G.; Pirani, F. *Chem. Phys. Lett.* **1991**, *183*, 297.
(41) Cambi, R.; Cappelletti, D.; Liuti, G.; Pirani, F. *J. Chem. Phys.* **1991**, *95*, 1852.
(42) Pirani, F.; Cappelletti, D.; Liuti, G. *Chem. Phys. Lett.* **2001**, *350*, 286.
(43) Denbigh, K. G. *Trans. Faraday Soc.* **1940**, *36*, 936. Hirschfelder, J. O.; Curtiss, C. F. M; Bird, R. B. *Molecular Theory of Gases and Liquids*; Wiley: New York, 1967.
(44) Maitland, G. C.; Rigby, M.; Smith, E. B.; Wakeham, W. A. *Intermolecular Forces*; Oxford University Press: New York, 1987.
(45) Sunner, J.; Nishizawa, K.; Kebarle, P. *J. Phys. Chem.* **1981**, *85*, 1814.
(46) Luhmer, M. K.; Dejaegere, A.; Bovy, P.; Reisse, J. *Bull. Soc. Chim. Fr.* **1994**, *131*, 603.
(47) Doerksen, R. J.; Thakkar, A. J. *J. Phys. Chem. A* **1999**, *103*, 10009.
(48) Choi, H. S.; Suh, S. B.; Cho, S. J.; Kim, K. S. *Proc. Natl. Acad. Sci. U.S.A.* **1998**, *95*, 12094.
(49) Feller, D.; Dixon, D. A.; Nicholas, J. B. *J. Phys. Chem. A* **2000**, *104*, 11414.
(50) De Wall, S. L.; Meadows, E. S.; Barbour, L. J.; Gokel, G. W. *Commun. PNAS* **2000**, *97*, 6271.